NANO LETTERS

2008
Vol. 8, No. 7
1798-1802

Surface Effect on the Elastic Behavior of Static Bending Nanowires

Jin He and Carmen M. Lilley*

Department of Mechanical and Industrial Engineering, University of Illinois at Chicago, 842 W. Taylor Street, Chicago, Illinois 60607

Received December 19, 2007; Revised Manuscript Received March 11, 2008

ABSTRACT

The surface effect from surface stress and surface elasticity on the elastic behavior of nanowires in static bending is incorporated into Euler−Bernoulli beam theory via the Young−Laplace equation. Explicit solutions are presented to study the dependence of the surface effect on the overall Young's modulus of nanowires for three different boundary conditions: cantilever, simply supported, and fixed−fixed. The solutions indicate that the cantilever nanowires behave as softer materials when deflected while the other structures behave like stiffer materials as the nanowire cross-sectional size decreases for positive surface stresses. These solutions agree with size dependent nanowire overall Young's moduli observed from static bending tests by other researchers. This study also discusses possible reasons for variations of nanowire overall Young's moduli observed.

Typically, nanowire (NW) elastic mechanical deformation modeling with atomistic simulations are for NWs in longitudinal extension. These atomistic simulations predict size dependent elastic behavior for NWs with cross-sectional sizes less than ~10 nm and almost constant elastic properties when NW cross-sectional sizes increasingly approach ~10 nm.[1,2] However, NWs are usually reported as bending mechanical structures in device applications such as actuators.[3] Both static[4–9] and dynamic bending tests[9,10] have been widely reported to characterize the elastic moduli of NWs made from various materials with different geometric sizes. For static bending tests, NWs exhibit a varying elastic modulus with respect to the cross-sectional sizes according to the experimentally measured force-displacement curves.[4–9] In these experiments, the cross-sectional sizes for the NWs range from 15 nm to several hundred nanometers. The origin of the experimentally observed size dependent elastic modulus of these NWs tested in static bending has been widely studied. In this paper, we will present an alternative approach using the Young−Laplace equation to study the influence of surface stress and surface elasticity effects on the static bending of NWs.

Surface stress and surface elasticity have been recognized as important factors that may explain the experimentally measured size dependent elastic modulus of NWs.[4,10–12] Several analytical approaches have been proposed to incorporate these surface effects into the Euler−Bernoulli law for elementary beam theory to investigate the elastic behavior of bending NWs.[4,10–12] Miller et al.[11] derived an expression from atomistic simulations to describe the effect of surface elasticity on the overall Young's modulus of NWs. Chen et al.[10] modeled the NW as a core−shell composite structure. The shell component is coaxial with the core and has a constant depth and Young's modulus different from the bulk value. Conversely, the proposed work outlined here assumes that the depth of the shell is negligible compared with the diameter of the NW and includes a surface stress to study size effects on measured elastic properties of NWs in static bending.

Cuenot et al.[12] introduced surface stress to study the NW bending behavior. Jing et al.[4] employed both the surface stress and the surface elasticity in his formulation. The expression given by Miller et al. is a special case of Jing's formula by neglecting the longitudinal extension of the NWs, and the equation by Cuenot et al. is similar to Jing's formula if the surface elasticity is neglected.[4] All of these approaches have the same foundation: the overall elastic behavior of NWs is a superposition of surface areas and the bulk volume where the bulk volume exhibits the identical elastic properties as the corresponding macroscopic bulk material. It should be noted that experimentally measured elastic moduli of NWs may not be independent of geometric sizes or shape and thus are not necessarily a material intrinsic property. In particular, at the nanoscale, intrinsic properties, such as Young's modulus, may not be directly measured because of the presence of the surface stress and surface elasticity in addition to geometric size and shape influences. Therefore, the experimentally measured elastic modulus has been referred to as the apparent Young's modulus,[4] the effective Young's modulus,[10] and Young's modulus.[9] For clarity with further discussions in this paper, the overall Young's modulus E_{ov} will be used for the experimentally measured elastic modulus, and Young's modulus E will be used for the intrinsic elastic modulus of the NWs.

* Corresponding author. E-mail: clilley@uic.edu.

10.1021/nl0733233 CCC: $40.75
Published on Web 05/30/2008

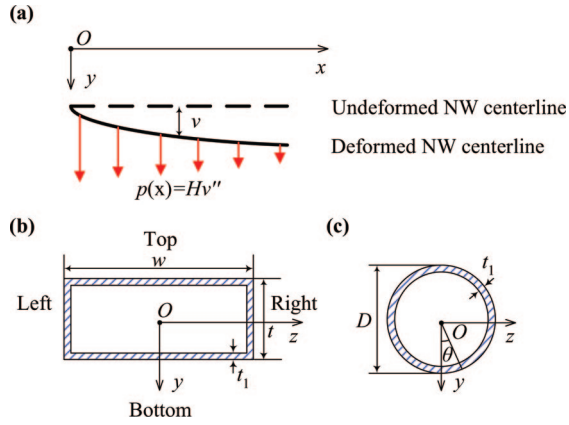

Figure 1. (a) Undeformed and deformed NW centerline. (b) Cross-sectional view of rectangular NW. (c) Cross-sectional view of circular NW.

In this paper, the surface effect on the elastic behavior of the static bending NWs is treated differently from the existing approaches by resorting to the generalized Young−Laplace equation.[13] This is also based on a continuum mechanics approach, and therefore, the developed theory is not applicable to ultra thin NWs such as those with $D < \sim 15$ nm as discussed by ref 14. The physical origin of the surface effect arises from bulk atoms imposing a stress constraint on the surface atoms due to the uncoordinated surface atoms.[15] A distributed transverse force results from the surface stress and acts on the NW in bending as described by the generalized Young−Laplace equation. The influence of longitudinal stress on the elastic bending behavior of NWs is assumed to be much smaller than the distributed transverse force. In addition, longitudinal extension of NWs is neglected, and small transverse displacement and deformation are used as an approximation. The Euler−Bernoulli equation is employed to incorporate the distributed transverse force, and concise theoretical solutions have been derived for cantilever, simply supported, and fixed−fixed bending NWs under a concentrated load. The obtained solutions are used to study how the surface stress influences the elastic bending behavior of NWs, where the surface stress may cause NWs to deform as softer or stiffer materials when compared with deformations calculated with Young's modulus. The theoretical solutions given in this paper are also compared with the size dependent NW overall Young's modulus observed from static bending tests by other researchers.[4,5,12] On the basis of the theoretical solutions, a possible reason for variations of NW overall Young's moduli observed in static bending tests reported from literature[6–9] is discussed.

The generalized Young−Laplace equation gives a mathematical description of the out-of-plane stresses induced from in-plane stresses of the curved interface surfaces:[11,13,16]

$$\Delta\sigma_{ij} n_i n_j = \tau_{\alpha\beta}\kappa_{\alpha\beta} \qquad (i,j=1,2,3;\alpha,\beta=1,2) \tag{1}$$

where $\Delta\sigma_{ij}$ is the stress jump across an interface surface, n_i is the unit vector normal to the surface, $\tau_{\alpha\beta}$ is the surface stress tensor, and $\kappa_{\alpha\beta}$ is the curvature tensor. For bending NWs in the y direction under small deformation as shown in Figure 1a, the stress jump described by eq 1 results in a distributed transverse force along the NW longitudinal direction:[16]

$$p(x) = Hv'' \tag{2}$$

where v is the NW transverse displacement, and H is a constant parameter which is determined by the surface stress along the NW longitudinal direction and the NW cross-sectional contour. The following notations will be used here for $v' = dv/dx$, $v'' = d^2v/dx^2$, $v''' = d^3v/dx^3$, and $v^{iv} = d^4v/dx^4$. For a rectangular NW, as shown in Figure 1b, the left and right surfaces do not contribute a distributed transverse force on the NW. For a circular NW, as shown in Figure 1c, the surface stress contributes a resultant transverse force along the y direction from the left and right semicircles. The parameter H for a rectangular[16] and circular cross sections is given by

$$H = \begin{cases} 2\tau w & \text{(Rect.)} \\ 2\int_{-\pi/2}^{\pi/2} D/2\tau\cos\theta \mathrm{d}\theta = 2\tau D & \text{(Circular)} \end{cases} \tag{3}$$

where w, t are width and thickness of the rectangular NWs respectively, D is the diameter of the circular NWs, and τ is the surface stress given by:[11]

$$\tau = \tau^0 + E_s\varepsilon_x \tag{4}$$

where τ^0 is the surface stress along NW longitudinal direction, E_s is the surface elastic modulus, and ε_x is the longitudinal strain of the surface caused by an applied force to the NW. The NWs are modeled as a superposition of surface layers and bulk volume, which is the same as previously introduced approaches in refs 4, 10, and 12. The shaded areas in Figure 1b,c represent the surface layers with an elastic modulus E_1 and thickness t_1. The thickness t_1 is assumed to be much smaller than the thickness t and the diameter D. The relationship between E_1 and E_s is $E_s = E_1 t_1$.[16] By using the composite beam theory[17] under the assumptions of $t_1 \ll t$ and $t_1 \ll D$, the effective bending modulus is

$$(EI)^* = \begin{cases} EI_1 + 2E_1(t/2)^2 w t_1 + 2E_1\int_{-\frac{t}{2}}^{\frac{t}{2}} y^2 t_1 dy \\ = EI_1 + \frac{1}{2}E_s w t^2 + \frac{1}{6}E_s t^3 & \text{(Rect.)} \\ EI_2 + E_1\int_0^{2\pi} [(D/2)\cos\theta]^2 (D/2) t_1 d\theta \\ = EI_2 + \frac{\pi}{8}E_s D^3 & \text{(Circular)} \end{cases} \tag{5}$$

where $I_1 = wt^3/12$ and $I_2 = \pi D^4/64$ are the moment of inertia of the rectangular and circular cross sections, respectively. The equilibrium equation for the bending NW under the distributed force is[17]

$$(EI)^* v^{iv} = p(x) \tag{6}$$

By substituting eqs 2–4 into eq 6 and using small deformation approximations $\varepsilon_x \approx -(t/2)v''$ and $\varepsilon_x \approx -(D/2)v''$ for rectangular and circular NWs respectively, eq 6 can be simplified to

$$(EI)^* v^{iv} = \begin{Bmatrix} 2[\tau^0 - E_s(t/2)v'']wv'' \\ 2[\tau^0 - E_s(D/2)v'']Dv'' \end{Bmatrix} \approx H^0 v'' \tag{7}$$

where the component of $(v'')^2$ is neglected for small deformation, and H^0 is similar to the definition of eq 3 except that τ^0 is substituted for τ.

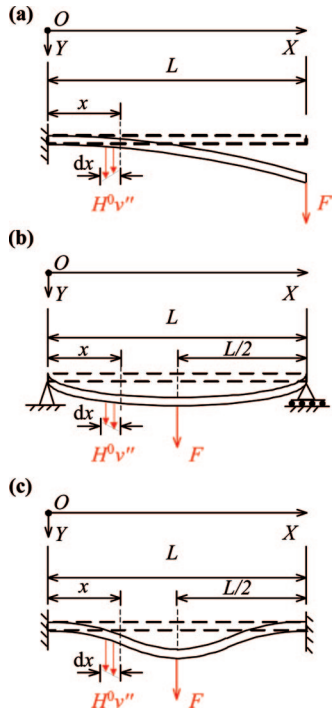

Figure 2. Illustration of bending NWs with different boundary conditions: (a) cantilever, (b) simply supported, (c) fixed−fixed.

Equation 7 is solved for three different boundary conditions: cantilever, simply supported, and fixed−fixed by using the approximated distributed transverse force H^0. An illustration of the boundary conditions and loading conditions is presented in Figure 2.

A constant concentrated load F is applied at the free end $x = L$ for the cantilever NW and at the midpoint $x = L/2$ for the simply supported and fixed−fixed NWs. For the cantilever NW, as shown in Figure 2a, at $x = 0$, the transverse displacement and slope are zeros resulting in $v_{(0)} = v'_{(0)} = 0$; the moment equilibrium condition is

$$(EI)^* v''_{(0)} = FL + \int_0^L H^0 v'' x dx = FL + H^0 L v'_{(L)} - H^0 v_{(L)} \quad (8)$$

and the force equilibrium condition is

$$-(EI)^* v'''_{(0)} = F + \int_0^L H^0 v'' dx = F + H^0 v'_{(L)} \quad (9)$$

For the simply supported NW, as shown in Figure 2b, at $x = 0$, the transverse displacement and bending moment are zeros resulting in $v_{(0)} = v''_{(0)} = 0$; the slope at $x = L/2$ is zero resulting in $v'_{(L/2)} = 0$ because of symmetry, and the force equilibrium at $x = 0$ is

$$-(EI)^* v'''_{(0)} = F/2 + \int_0^{L/2} H^0 v'' dx = F/2 - H^0 v'_{(0)} \quad (10)$$

For the fixed−fixed NW, as shown in Figure 2c, the boundary condition is the same as the cantilever NW at $x = 0$, the slope is the same as the simply supported NW at $x = L/2$, and the force equilibrium at $x = 0$ is

$$-(EI)^* v'''_{(0)} = F/2 + \int_0^{L/2} H^0 v'' dx = F/2 \quad (11)$$

The solutions to eq 7 with the aforementioned concentrated load and boundary conditions are given by eq 12a for $H^0 = 0$ and eq 12b for $H^0 \neq 0$, respectively. The equations shown in eq 12a have the same form of solutions as found in the classical Euler−Bernoulli theory[17] by neglecting E_s. The nondimensional surface effect factor $\eta = H^0 L^2/(EI)^*$ is introduced here to simplify the solutions shown in eq 12b. The surface effect factor reflects the extent to which the surface effect influences the overall elastic behavior of the static bending NWs. The value of η can be either positive or negative because of the positive and negative τ_0 reported from atomistic simulations.[18] The surface effect diminishes for a smaller absolute value of the surface effect factor and can be neglected when η approaches zero. As η approaches zero, eq 12b gives the same results as shown in eq 12a when $H^0 = 0$.

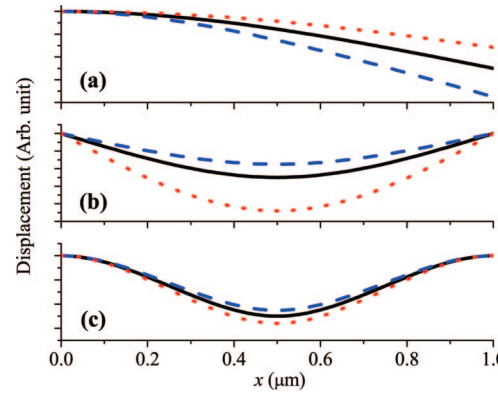

Figure 3. Transverse displacement along NW longitudinal direction with different boundary conditions: (a) cantilever, (b) simply supported, (c) fixed−fixed. Black solid line: $\tau_0 = 0$. Blue dashed line: $\tau_0 = 1$ μN/μm. Red dotted line: $\tau_0 = -1$ μN/μm.

When $H^0 = 0$, then

$$v = \begin{cases} \dfrac{F(3L - x)x^2}{6(EI)^*}, & x \in [0, L] \quad \text{(cantilever)} \\ \dfrac{F(3L^2 - 4x^2)x}{48(EI)^*}, & x \in [0, L/2] \quad \text{(simple)} \\ \dfrac{F(3L - 4x)x^2}{48(EI)^*}, & x \in [0, L/2] \quad \text{(fixed - fixed)} \end{cases} \quad (12a)$$

and when $H^0 \neq 0$, then

$$v = \begin{cases} \dfrac{F\cosh\sqrt{\eta}}{H^0}\left[x - \dfrac{L}{\sqrt{\eta}}\tanh\sqrt{\eta} - \dfrac{L}{\sqrt{\eta}}\dfrac{\sinh(\sqrt{\eta}x/L - \sqrt{\eta})}{\cosh\sqrt{\eta}}\right], \\ \qquad x \in [0, L] \quad \text{(cantilever)} \\ \dfrac{F}{2H^0}\left[x - \dfrac{L}{\sqrt{\eta}}\dfrac{\sinh(\sqrt{\eta}x/L)}{\cosh(\sqrt{\eta}/2)}\right], \\ \qquad x \in [0, L/2] \quad \text{(simple)} \\ \dfrac{F}{2H^0}\left[x - \dfrac{L}{\sqrt{\eta}}\tanh(\sqrt{\eta}/4) - \dfrac{L}{\sqrt{\eta}}\dfrac{\sinh(\sqrt{\eta}x/L - \sqrt{\eta}/4)}{\cosh(\sqrt{\eta}/4)}\right], \\ \qquad x \in [0, L/2] \quad \text{(fixed - fixed)} \end{cases} \quad (12b)$$

Example calculations are shown in Figure 3 for eqs 12a and 12b for circular NWs. The modeling parameters are $L = 1$ μm, $D = 50$ nm, $E = 76$ GPa, and $E_s = 0$. It can be seen that the cantilever NW exhibits a softer elastic behavior while the simply supported and fixed−fixed NWs exhibit a stiffer elastic behavior for $\tau_0 > 0$ (and vice versa for $\tau_0 <$

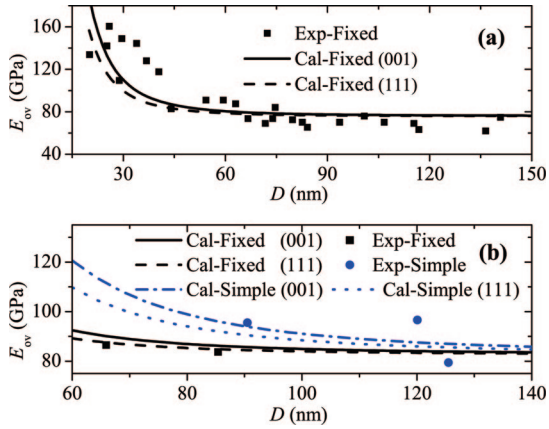

Figure 4. Overall Young's modulus versus diameter of silver NWs. (a) Fixed−fixed NWs. Experimental data are from ref 4. (b) Fixed−fixed and simply supported NWs. Experimental data are from ref 5.

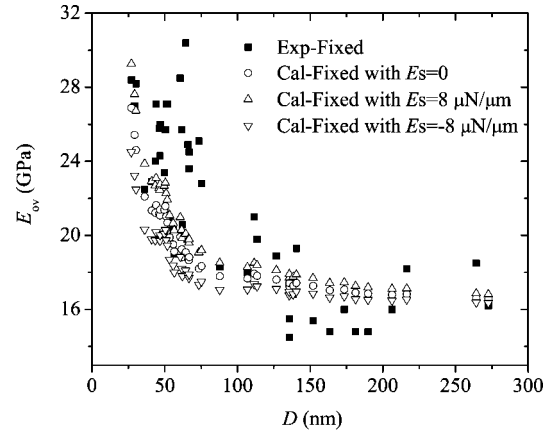

Figure 5. Overall Young's modulus versus diameter of lead NWs. Experimental data are from ref12.

0) than the corresponding NWs without the surface effect. The stiffer or softer behavior is attributed to the signs of the curvature and surface stress during the static bending of the NWs. The downward curvature, as shown in Figure 3a for the cantilever NWs, results in a positive curvature. According to eq 2, a positive curvature results in a positive distributed transverse force in the same direction with the external load if $\tau_0 > 0$. Thus, the distributed transverse force increases the transverse displacement of the bending NW and the cantilever NW behaves like a softer material. Conversely, an upward curvature occurs in the simply supported NWs, as shown in Figure 3b, resulting in a negative curvature. In this case, the distributed force caused from the positive surface stress mitigates the external load and decreases the transverse displacement of the NW. Hence, the simply supported NW behaves like a stiffer material. Both downward and upward curvatures occur in the fixed−fixed NW as shown in Figure 3c with a similar trend of stiffer/softer behavior as in the simply supported NW. This implies that the upward curvature region has a greater influence on the elastic deformation because the NW behaves like a stiffer material if $\tau_0 > 0$. If the downward curvature was dominant, then the NW would have appeared to be a softer material for $\tau_0 > 0$. For a given surface effect factor η, the surface effect has less influence on the stiffer/softer behavior of the fixed−fixed NW than the simply supported NW because of the counteraction of the positive and negative distributed transverse force for the fixed−fixed NW.

Equations 12a and 12b have also been applied to explain the experimentally measured size dependent overall Young's moduli of silver NWs[4,5] and lead NWs[12] as reported from literature. Experimental results are compared with theoretical calculations as shown in Figure 4 and Figure 5 for silver and lead NWs, respectively. The theoretically calculated overall Young's moduli are obtained by solving for E from eq 12a with $E_s = 0$ and at $x = L/2$ for the simply supported and fixed−fixed NWs. The transverse displacement v used in eq 12a is calculated from eq 12b at the same location. For the theoretical calculations with (001) and (111) silver, surface stress and surface elasticity values from atomistic calculations of $\tau_0 = 0.89$ μN/μm, $E_s = 1.22$ μN/μm, and $\tau_0 = 0.65$ μN/μm, $E_s = -1.39$ μN/μm were used respectively in eq 12b.[18] The surface elastic modulus E_s is calculated from surface elastic constants S_{1111}, S_{1122} given in ref 18 by using $E_s = (S_{1111} + 2S_{1122})(S_{1111} - S_{1122})/(S_{1111} + S_{1122})$. To the best of our knowledge, there are no published values of E_s for lead. Therefore, different values of E_s were assumed in Figure 5. The value of $\tau_0 = 0.63$ μN/μm for (001) and (111) lead calculated from atomistic simulations[19] was used. The silver NW length L used in the theoretical calculations is 1 μm and 1.5 μm for Figure 4a,b, respectively. The lengths for the lead NWs were not uniform in the experiments found in ref 12 and the measured lengths L for each lead NW were used in the theoretical calculations. For refs 4 and 5, the researchers cite silver Young's modulus values of $E = 76$ GPa[4] and $E = 82.7$ GPa,[5] respectively. These same values are used for the calculations shown in the respective graphs of Figure 4. Also, the same Young's modulus of $E = 16$ GPa for lead as given in ref 12 was used for the calculations shown in Figure 5.

As can be seen in Figure 4a, the general trend of the overall Young's modulus for silver NWs is increasing with decreasing diameter when the NW length is constant for both the experimental results and the proposed theory. The experimental results from ref 5, as shown in Figure 4b, are obtained for both simply supported and fixed−fixed NWs. However, the experimentally measured overall Young's modulus does not increase as the NW diameter decreases, and there is a decrease of the overall Young's modulus for the two smallest cross-sectional NWs. These seemingly scattered experimental results can be explained by different boundary conditions of NWs employed in the experiment. When the NW diameter decreases, the increment of the overall Young's modulus for the fixed−fixed NW is lower than the simply supported NWs as predicted by the theoretical calculations, and thus smaller simply supported NWs may exhibit a lower overall Young's modulus than larger fixed−fixed NWs. An underlying cause can be explained as a lower influence from the surface effect on the static bending behavior of the fixed−fixed NW than the simply supported NWs. Finally, as seen in Figure 5, the trend of E_{ov} of lead NWs from theoretical calculations is

also similar to the experimental results. The scattered theoretical calculation data points shown in Figure 5 are due to the varying experimentally measured NW lengths used in the calculations. As can also be seen, the theoretical calculations with assumed positive E_s predict higher E_{ov} than those with negative E_s. In summary, the theoretical calculations agree with the experimental results shown in Figure 4 and Figure 5 and may provide an explanation of the scattered experimental results shown in Figure 4b.

Furthermore, the theoretical results presented in this paper provide a guide to understanding the origin of the varied overall Young's modulus of NWs reported from literature. For example, the overall Young's modulus of a cantilever NW has been measured to be lower than the fixed−fixed NW for the static bending tests of silicon NWs.[9] Similar observations have been found for zinc oxide NWs, where cantilever zinc oxide NWs[6] have lower overall Young's moduli than those of the fixed−fixed NWs.[7] These results can be explained by the proposed theoretical results under the assumption that positive surface stresses occur in these NWs. However, the overall Young's moduli of the "fixed−fixed" zinc oxide NWs reported from ref 8 show much lower values than the simply supported NWs reported from ref 7. A possible reason for these contradictory experimental results is that the boundary conditions for the NWs employed in ref 8 may not be fixed−fixed but simply supported. At the midpoint $x = L/2$, the overall Young's modulus is $E_{ov} = FL^3/[48(EI)^*v]$ for the simply supported and $E_{ov} = FL^3/[192(EI)^*v]$ for the fixed−fixed NWs, as obtained from eq 12a. Therefore, the actual E_{ov} is four times larger if the simply supported NWs are misunderstood as the fixed−fixed NWs. The importance of recognizing the real boundary conditions for static bending NWs has already been emphasized by some researchers,[5,7] and in these experiments, the in situ recording of the transverse displacement profile along x direction is used to determine the real boundary conditions of the bending NWs. The single crystal structure for silicon (diamond cubic) and zinc oxide (wurtzite) NWs are more complex than those of silver and lead which are face center cubic. As a result, varying surface stress values have been calculated with atomistic simulations. For example, a wide range of positive to negative surface stress values for silicon has been reported in refs 11, 15, and 20. Researchers have also found that the E_{ov} of zinc oxide NWs may be influenced by a piezoelectric mechanical effect. Although the influence from the piezoelectric mechanical interaction on E_{ov} has not been mentioned for static bending ZnO NWs, the piezoelectric phenomenon was found to influence the longitudinal deformation of zinc oxide NWs by Desai et al.[21] As a result, modeling these more complex structures with the proposed theory in this paper are their own scope of work, and further research is needed. Extension of our approach from the static bending NWs to dynamic bending NWs is in progress.

Finally, it should be pointed out that the surface effect factor η indicates a magnitude of the influence of the surface effect on the overall Young's modulus of NWs. The surface effect factor η can be approximated as $24(\tau^0/E)\cdot(L^2/t^3)$ and $(128/\pi)\cdot(\tau^0/E)\cdot(L^2/D^3)$ for rectangular and circular NWs respectively by neglecting E_s. The term $(\tau^0/E)\cdot(L^2/D^3)$ has also appeared in Jing's[4] and Cuenot's[12] approaches. The theoretical approach presented in this paper suggests that, in contrast to a width-to-thickness ratio or a surface-to-volume ratio as presented in ref 8, the overall Young's modulus E_{ov} should be studied as a function of the surface effect factor η because of the direct influence of η on E_{ov} for static bending NWs.

In summary, the influence of the surface effect from the surface stress and the surface elasticity on the static bending behavior of NWs was investigated by resorting to the Young−Laplace equation. The analytical approach presented in this paper provides explicit solutions for NWs with three different boundary conditions: cantilever, simply supported, and fixed−fixed. The solutions indicate that the cantilever NWs behave as softer materials when deflected while the other structures behave like stiffer materials as the NW cross-sectional size decreases for positive surface stresses. These results provide insight to the possible cause of variation in experimentally measured overall Young's moduli for silicon and zinc oxide NWs. These solutions also agree with the size dependent NW overall Young's moduli observed from static bending tests for silver and lead NWs. The presented approach suggests that the overall Young's modulus of NWs should be studied as a function of the surface effect factor.

Acknowledgment. The authors wish to express our gratitude to Dr. Bernard Nysten from Université Catholique de Louvain, Belgium for his valuable input on the experimental results found in ref 12 and in Figure 5 of this paper.

References

(1) Diao, J. K.; Gall, K.; Dunn, M. L. *J. Mech. Phys. Solids* **2004**, *52*, 1935.
(2) Wu, H. A. *Mechanics Research Communications* **2006**, *33*, 9.
(3) Feng, X. L.; He, R. R.; Yang, P. D.; Roukes, M. L. *Nano Lett.* **2007**, *7*, 1953.
(4) Jing, G. Y.; Duan, H. L.; Sun, X. M.; Zhang, Z. S.; Xu, J.; Li, Y. D.; Wang, J. X.; Yu, D. P. *Phys. Rev. B* **2006**, *73*, 235409.
(5) Chen, Y. X.; Dorgan, B. L.; McIlroy, D. N.; Aston, D. E. *J. Appl. Phys.* **2006**, *100*, 104301.
(6) Song, J. H.; Wang, X. D.; Riedo, E.; Wang, Z. L. *Nano Lett.* **2005**, *5*, 1954.
(7) Mai, W. J.; Wang, Z. L. *Appl. Phys. Lett.* **2006**, *89*, 073112.
(8) Ni, H.; Li, X. O. *Nanotechnology* **2006**, *17*, 3591.
(9) Tabib-Azar, M.; Nassirou, M.; Wang, R.; Sharma, S.; Kamins, T. I.; Islam, M. S.; Williams, R. S. *Appl. Phys. Lett.* **2005**, *87*, 113102.
(10) Chen, C. Q.; Shi, Y.; Zhang, Y. S.; Zhu, J.; Yan, Y. J. *Phys. Rev. Lett.* **2006**, *96*, 075505.
(11) Miller, R. E.; Shenoy, V. B. *Nanotechnology* **2000**, *11*, 139.
(12) Cuenot, S.; Fretigny, C.; Demoustier-Champagne, S.; Nysten, B. *Phys. Rev. B* **2004**, *69*, 165410.
(13) Chen, T. Y.; Chiu, M. S.; Weng, C. N. *J. Appl. Phys.* **2006**, *100*, 074308.
(14) Govindjee, S; Sackman, J. L. *Solid State Commun.* **1999**, *110*, 227.
(15) Cammarata, R. C.; Sieradzki, K. *Annu. Rev. Mater. Sci.* **1994**, *24*, 215.
(16) Wang, G. F.; Feng, X. Q. *Appl. Phys. Lett.* **2007**, *90*, 231904.
(17) Gere, J. M.; Timoshenko, S. P. *Mechanics of Materials*; Wadsworth International: CA, 1985.
(18) Shenoy, V. B. *Phys. Rev. B* **2005**, *71*, 094104.
(19) Wan, J.; Fan, Y. L.; Gong, D. W.; Shen, S. G.; Fan, X. Q. *Modelling Simul. Mater. Sci. Eng.* **1999**, *7*, 189.
(20) Lee, B.; Rudd, R. E. *Phys. Rev. B* **2007**, *75*, 195328.
(21) Desai, A. V.; Haque, M. A. *Appl. Phys. Lett.* **2007**, *91*, 183106.

NL0733233